American Mineralogist, Volume 72, pages 821–831, 1987

(Sb,Bi,Pb) ordering in sulfosalts: Crystal-structure refinement of a Bi-rich izoklakeite

THOMAS ARMBRUSTER, WOLFGANG HUMMEL
Laboratorium für chemische und mineralogische Kristallographie der Universität Bern, Freiestrasse 3, CH-3012 Bern, Switzerland

ABSTRACT

The crystal structure of a Bi-rich izoklakeite, $Cu_{2.6}Fe_{1.4}Ag_{0.9}Pb_{53.8}Bi_{22.6}Sb_{14.8}S_{114}$, space group *Pnnm*, Z = 1, $a = 34.221(8)$, $b = 37.933(8)$, $c = 4.063(3)$ Å was refined from X-ray single-crystal data to $R = 5.9\%$, $R_w = 7.3\%$. The specimen was originally included in a quartz crystal and was found near Lake Zervreila, Graubünden, Switzerland. The specimen's crystal structure is composed of PbS- and SnS-like units and thus is in fair agreement with the structure of Sb-rich izoklakeite from Vena, Sweden (Makovicky and Mumme, 1986). The distribution of Sb-rich atomic positions is determined by site-occupancy refinements. Because Bi^{3+} and Pb^{2+} are isoelectronic and cannot be distinguished by their X-ray scattering behavior, a Me–S distance reference diagram for Sb–S, Bi–S, Pb–S, and Tl–S is herein developed on the basis of literature data. Mean Me–S bond lengths are not applicable to sulfosalts owing to the strong distortions of the coordination polyhedra caused by the lone electron pairs characteristic of these ions. A diagram where the mean value of the three shortest Me–S distances is plotted versus the mean value of the next two shortest ones seems suitable to distinguish Sb^{3+}, Bi^{3+}, Pb^{2+}, and Tl^{+}. (Pb,Bi)-bearing sulfosalt structures given in the literature are tested with this diagram. The izoklakeite investigated possesses 1 pure Sb site, 10 mixed (Bi,Sb) sites with additional Pb, 2 mixed (Bi,Pb) sites, and 10 Pb sites. Cu and Fe occupy a fourfold-coordinated position. Ag could not be localized, but probably replaces Pb according to the substitution $Bi^{3+} + Ag^{+} \rightarrow 2Pb^{2+}$.

INTRODUCTION

Izoklakeite and giessenite are rare sulfosalts containing Pb, Bi, and Sb and to a lesser extent Cu, Fe, and Ag. Both minerals have been derived as members with $N = 4$ of the kobellite homologous series (Makovicky and Mumme, 1986). From a chemical point of view, giessenites show only low Sb concentrations [Graeser and Harris, 1986: Sb/(Bi + Sb) = 0.195; Makovicky and Karup-Møller, 1986: Sb/(Bi + Sb) = 0.148], whereas izoklakeite is richer in Sb [Makovicky and Mumme, 1986: Sb/(Bi + Sb) = 0.511; Harris et al., 1986: Sb/(Sb + Bi) = 0.527]. Although quite similar in unit-cell dimensions, giessenites are monoclinic and izoklakeites are orthorhombic. Up until recently, there has been some controversy over whether the correct crystal system of giessenite is also orthorhombic with space group $P2_12_12_1$ (Graeser, 1963; Karup-Møller, 1973) or only monoclinic ($P2_1/n$), but intimately twinned (Makovicky, 1981; Makovicky and Mumme, 1986).

Giessenite (Table 1) was first described by Graeser (1963) from the Binnatal (Wallis, Switzerland), and the name was chosen after a small hamlet close to the sulfosalt-bearing dolomite outcrop. A second occurrence was reported by Karup-Møller (1973) from the Bjorkåsen sulfide deposit at Otoften in northern Norway. At this stage we were studying an orthorhombic mineral (space group *Pnnm*), similar to giessenite but richer in Sb (Table 1), which was found as inclusions in quartz from Lake Zervreila (Vals, Graubünden, Switzerland) (Armbruster et al., 1984). The IMA Commission on New Minerals and Mineral Names informed us that the mineral species proposed by us was identical either with a new mineral called izoklakeite (not yet published at that time) or with giessenite, for which the space group had not been clearly defined. Thus we named the mineral Sb-rich giessenite. Recent reinvestigations of the giessenites from Binnatal and from Bjorkåsen proved both to be monoclinic with the space group $P2_1/n$, Z = 1, $a = 34.5$, $b = 38.18$, $c = 4.08$ Å, $\beta = 90°$ (Graeser and Harris, 1986; Makovicky and Karup-Møller, 1986).

Izoklakeite [ideal formula: $(Cu,Fe)_4Pb_{54}(Sb,Bi)_{38}S_{114}$] is an orthorhombic sulfosalt with $a = 33.88(2)$, $b = 38.02(2)$, $c = 4.070(2)$ Å, first described by Harris et al. (1986) from the massive zinc-copper-lead sulfide deposit at Izok Lake, Northwest Territories (Canada). A second occurrence (Table 1) was reported by Zakrzewski and Makovicky (1986) from the abandoned vena copper-cobalt mine, Bergslagen, Sweden. Makovicky and Mumme (1984, 1986) solved the structure of izoklakeite using a specimen from Bergslagen. The crystal structure [*Pnnm*, $a = 34.07(1)$, $b = 37.98(1)$, $c = 4.072(1)$ Å, Z = 1 on the basis of 114 S] was refined from X-ray single-crystal data to an R value of 16% with 1434 reflections (Makovicky and Mumme, 1986).

0003–004X/87/0708–0821$02.00

TABLE 1. Chemical formulae of giessenites and izoklakeites from various localities

Locality	Cu	Fe	Ag	Pb	Bi	Sb	S	References
					Giessenites			
Binnatal, Switzerland	4.3	—	—	51.8	32.2	7.8	114 (116.2)	Graeser and Harris, 1986
Bjorkåsen, Norway	3.4	0.4	0.2	52.8	33.4	5.8	114	Makovicky and Karup-Møller, 1986
					Izoklakeites			
Izok Lake, Canada	3.2	0.7	3.8	45.9	20.0	22.3	114 (108.3)	Harris et al., 1986
Bergslagen, Sweden	2.9	0.7	1.2	51.3	19.5	20.4	114 (112.1)	Zakrzewski and Makovicky, 1986
Zervreila Lake, Switzerland	2.6	1.4	0.9	53.8	22.6	14.8	114 (117.3)	This paper

Note: Based on 96 cations; measured S concentration in parentheses.

Before the papers of Makovicky and Mumme (1984, 1986) appeared, we had collected single-crystal X-ray intensity data on the Zervreila "Sb-rich giessenite," which now should be classified as Bi-rich izoklakeite [Sb/(Bi + Sb) = 0.39], because it is orthorhombic rather than monoclinic like giessenite (Makovicky and Karup-Møller, 1986). All heavy atoms of this Bi-rich izoklakeite were localized by direct methods using the computer program MULTAN (Main et al., 1978). When we noticed that the structure was solved (Makovicky and Mumme, 1984) we abandoned this study. However, the poor quality of the refinement of the izoklakeite structure (Makovicky and Mumme, 1986) and the distinct difference in the Sb/(Sb + Bi) ratio between izoklakeite and giessenite motivated us to complete the structural investigation, which is presented in this paper.

EXPERIMENTAL DETAILS

A prismatic crystal (400 μm along **c**) bounded by ($\bar{1}10$), ($1\bar{1}0$), (130), and ($\bar{1}\bar{3}0$) faces (130 × 65 μm in diameter) was utilized for all X-ray measurements. The crystal composition $Cu_{2.6}Fe_{1.4}Ag_{0.9}Pb_{53.8}Bi_{22.6}Sb_{14.8}S_{114(117.3)}$ (standardized on 96 cations, measured S concentration in parentheses) was determined by electron microprobe (Armbruster et al., 1984). Oscillation photographs with Cu*Kα* radiation were used to find the **c** axis, and Weissenberg *hk*0, *hk*1 photographs served for the determination of **a** and **b**. The space group was identified to be either *Pnnm* or *Pnn*2. Makovicky and Karup-Møller (1986) interpreted the presence of 081, 0.10.1, 0.26.1, 0.28.1, 092, and 0.27.2 reflections as indicating the monoclinic $P2_1/n$ space group characteristic of giessenite. None of these reflections was observed for the sulfosalt investigated. All X-ray reflections, including those with high θ values, were extraordinarily sharp and did not reveal any indication of twinning. Overexposed oscillation photographs around the **c** axis displayed a very weak superstructure with c = 8 Å. Similar results were also reported for kobellite (Miehe, 1971) and izoklakeite (Makovicky and Mumme, 1986).

Collection of X-ray intensity data was performed with a CAD-4 single-crystal diffractometer using graphite-monochromated Mo*Kα* radiation. Cell dimensions were refined from the scattering vectors of 25 reflections (*hkl*: 30.0.0, 0.30.0, 006, 004, 753, 15.8.1, and their symmetry equivalents), yielding $a = 34.221(8)$ Å, $b = 37.933(8)$ Å, and $c = 4.063(3)$ Å. Intensities of 8700 reflections in one quadrant of reciprocal space were collected with an Ω scan mode up to $\theta = 30°$. To minimize absorption effects ($\mu_0 = 600$ cm^{-1}), a needle mode, which selects a crystal-scattering position with the highest transmission factor during intensity measurement, was chosen. Reflections for which a prescan found $\sigma(I)/I > 0.5$ were flagged as weak. The final scan speed of stronger reflections was calculated in order to obtain $\sigma(I)/I = 0.03$. Data reduction, including background and Lorentz-polarization corrections, was carried out with the SDP program system (Enraf-Nonius, 1983). An absorption correction was rejected, because the agreement factor between 200 test reflections (measured in an additional quadrant) and the symmetry-equivalent ones was not improved. Already at this stage we suspected that the crystal was also affected by strongly anisotropic extinction.

Reflections allowed under *Pnnm* symmetry were employed for the refinement of the structure using the starting values of Makovicky and Mumme (1986) with the program system PROMETHEUS (Zucker et al., 1983). Structure factors were weighted on the basis of counting statistics ($w = 1/\sigma^2$), applying a $6\sigma(F_{obs})$ cutoff. Neutral-atom scattering factors and real as well as imaginary parts of the anomalous dispersion corrections were used. In the first refinement cycles, the Sb,(Bi,Pb) distribution in each metal position was tested, by refining the Sb,(Bi,Pb) population. If the Sb concentration was found to be less than 2%, only (Pb,Bi) was assumed on this position. Cu and Fe were assigned to the fourfold-coordinated M(24) site. Because the program PROMETHEUS allows only 200 parameters to be refined simultaneously, a stepwise procedure was necessary. Atomic positions, selected Sb,(Bi,Pb) populations, anisotropic cation-displacement vectors, and isotropic S-displacement vectors were refined together, whereas in the following cycle, S positions and S-displacement parameters were refined. Subsequent cycles converged to R = 6.8% (R_w = 9.5%) on the basis of 3047 reflections. Comparison of observed and calculated structure factors (Table 2)[1] of strong reflections with high d values confirmed our assumption that the crystal was affected by anisotropic extinction. In turn, we introduced a lower sin θ/λ limit of 0.25 and refined the structure to R = 5.9% and R_w = 7.3% on the basis of 2779 reflections. Positional parameters, occupational parameters, and temperature factors of refinements with and without the sin θ/λ limit agree within $\pm 3\sigma$. Differences in the scattering behavior of Pb and Bi are so small that a distinction between these elements is not possible on this basis.

---

[1] To obtain a copy of Table 2, order Document Am-87-342 from the Business Office, Mineralogical Society of America, 1625 I Street, N.W., Suite 414, Washington, D.C. 20006, U.S.A. Please remit $5.00 in advance for the microfiche.

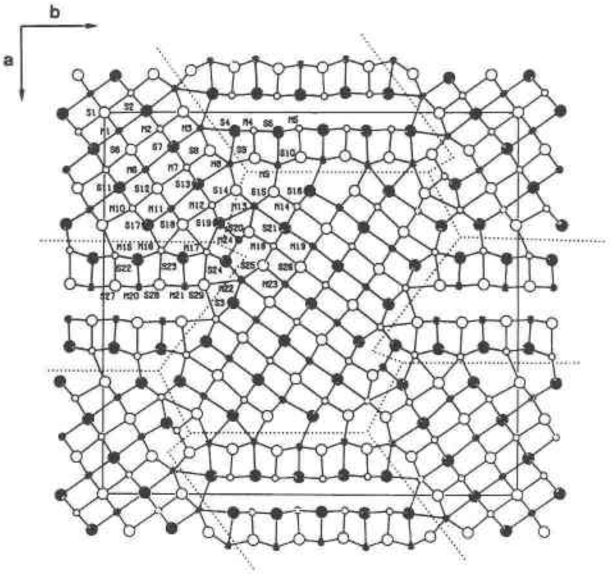

Fig. 1. (001) section of the crystal structure of Bi-rich izoklakeite. Small circles denote (Pb,Bi,Sb) positions coordinated by 5 to 8 S atoms (large circles). In addition, the fourfold-coordinated site M(24) (Cu,Fe) is also represented by a small circle. Filled circles are at $z = \pm 1/2$; open circles at $z = 0$. The structure is composed of galena-like blocks connected with SnS type units (Makovicky, 1985) that are characterized by open channels. The connection between the two different structural units (indicated by dotted lines) leads to uninterrupted noncommensurate interfaces (Makovicky and Mumme, 1986), which are made possible by the strong distortions and variations of SbS_n, BiS_n, and PbS_n coordination polyhedra.

TABLE 3. Final atomic positional parameters and B_{eq} values

Atom	x/a	y/b	z/c	B_{eq} (Å^2)
M1	0.04827(7)	0.03469(7)	0.5	1.43(5)
M2	0.04388(8)	0.13345(7)	0.0	1.23(6)
M3	0.04165(8)	0.23059(8)	0.5	1.77(5)
M4	0.04744(10)	0.35911(10)	0.0	2.02(8)
M5	0.04168(14)	0.46960(14)	0.0	4.0(1)
M6	0.15005(7)	0.09886(7)	0.5	1.45(4)
M7	0.14483(8)	0.19814(8)	0.0	1.37(6)
M8	0.13525(9)	0.30089(8)	0.5	2.20(5)
M9	0.13874(9)	0.41790(8)	0.5	2.07(5)
M10	0.25127(8)	0.06784(7)	0.0	1.54(5)
M11	0.25315(7)	0.16123(7)	0.5	1.50(4)
M12	0.24304(8)	0.25901(8)	0.0	1.32(6)
M13	0.24578(8)	0.36087(9)	0.5	2.43(6)
M14	0.24619(8)	0.46486(7)	0.0	1.37(6)
M15	0.37498(8)	0.02710(8)	0.0	2.05(5)
M16	0.36226(8)	0.13691(7)	0.0	1.80(5)
M17	0.36614(9)	0.24655(8)	0.0	2.29(5)
M18	0.35015(8)	0.40773(7)	0.0	1.62(5)
M19	0.35019(8)	0.50372(7)	0.5	1.42(4)
M20	0.45829(13)	0.08472(15)	0.5	2.0(1)
M21	0.45635(10)	0.19443(10)	0.5	2.18(8)
M22	0.43874(9)	0.33025(9)	0.0	2.33(5)
M23	0.44998(8)	0.43673(8)	0.5	1.51(6)
M24	0.3336(3)	0.3235(3)	0.5	1.8(2)
S1	0.0	0.0	0.0	3.8(7)*
S2	−0.0033(5)	0.1012(5)	0.5	2.0(3)*
S3	0.4989(4)	0.3107(4)	0.5	1.0(2)*
S4	0.0484(5)	0.3135(5)	0.5	2.1(3)*
S5	0.0514(5)	0.4184(5)	0.5	2.4(3)*
S6	0.0976(5)	0.0641(5)	0.0	1.7(3)*
S7	0.0903(5)	0.1656(5)	0.5	1.9(3)*
S8	0.1006(4)	0.2534(4)	0.0	1.3(3)*
S9	0.1203(5)	0.3617(5)	0.0	1.7(3)*
S10	0.1178(5)	0.4738(5)	0.0	1.6(3)*
S11	0.1964(5)	0.0365(5)	0.5	1.9(3)*
S12	0.1997(5)	0.1271(4)	0.0	1.4(3)*
S13	0.1881(5)	0.2253(5)	0.5	2.2(3)*
S14	0.2040(4)	0.3164(4)	0.0	1.4(3)*
S15	0.2077(4)	0.4078(4)	0.0	1.3(3)*
S16	0.2057(5)	0.4950(5)	0.5	2.3(4)*
S17	0.2951(5)	0.1048(4)	0.5	1.6(3)*
S18	0.2939(4)	0.1888(4)	0.0	1.2(3)*
S19	0.2894(5)	0.2754(5)	0.5	2.3(3)*
S20	0.3135(5)	0.3484(4)	0.0	1.6(3)*
S21	0.3023(5)	0.4352(5)	0.5	1.8(3)*
S22	0.3861(5)	0.0811(4)	0.5	1.3(3)*
S23	0.3821(5)	0.1890(4)	0.5	1.7(3)*
S24	0.3910(4)	0.2927(4)	0.5	1.2(3)*
S25	0.4008(5)	0.3827(5)	0.5	2.3(3)*
S26	0.4052(5)	0.4738(5)	0.0	2.1(3)*
S27	0.4542(5)	0.0281(5)	0.0	2.1(3)*
S28	0.4520(6)	0.1335(5)	0.0	2.7(4)*
S29	0.4519(5)	0.2402(4)	0.0	1.6(3)*

Note: Standard deviations in parentheses.

* Atoms that were refined isotropically. Anisotropically refined atoms are given in the form of the isotropic equivalent thermal parameter, defined as $B_{eq} = 8/3\pi^2 \Sigma_{ij}(U_{ij}a_i^* a_j^* a_i a_j)$. $\sigma(B_{eq})$: Schomaker and Marsh (1983).

RESULTS

According to Makovicky and Mumme (1986), the izoklakeite structure (Fig. 1) can best be described as being composed of two types of units that form endless rods parallel to the **c** axis. One rod type resembles a galena unit, the other a SnS-like arrangement (Makovicky, 1985). The latter type displays endless open channels running parallel to **c**. The individual units are connected by a distorted $(Cu,Fe)S_4$ tetrahedron [M(24)] and long Me–S bonds.

Although the general description of the izoklakeite structure (Makovicky and Mumme, 1986) is correct and in agreement with our results for a Bi-rich izoklakeite, the structural data of Makovicky and Mumme (1986) show several peculiarities. The positional errors of the relatively light S atoms are smaller than the positional errors of the heavier Sb, Bi, and Pb atoms, and the S atoms display isotropic temperature factors (B) ranging between 0.1(2) and 7.7(7). In addition, anisotropic temperature parameters for metal positions are only highly significant parallel to the **c** axis (β_{33}), whereas β_{11}, β_{22}, and β_{12} show values that are only 1 to 5 times larger than their standard deviation. In spite of these findings, Makovicky and Mumme (1986) interpreted some large thermal parameters of S as due to positional disorder on (Bi,Sb) and (Bi,Pb) sites. They also discussed the anisotropy of some thermal ellipsoids of the metals in terms of the positional separation of Bi and Sb.

In the refinement of the Bi-rich Lake Zervreila izoklakeite, the positional errors of the metals (Sb,Bi,Pb) are about 5 times smaller than those of S (Table 3), and are thus in agreement with theory. The isotropic temperature factors (B) of S range between 1.0 and 3.8, and the isotropic temperature-factor equivalents (B_{eq}) of the metal positions lie between 1.2 and 4.0 (Table 3). The errors of U_{11}, U_{22}, and U_{33} are of the same magnitude and about

TABLE 4. Thermal parameters

Atom	U_{11}	U_{22}	U_{33}	U_{12}
M1	0.019(1)	0.022(2)	0.013(1)	−0.003(1)
M2	0.015(2)	0.017(2)	0.015(2)	0.000(1)
M3	0.028(1)	0.025(1)	0.014(1)	−0.001(1)
M4	0.022(2)	0.030(2)	0.025(3)	0.000(1)
M5	0.066(4)	0.064(4)	0.023(3)	−0.039(3)
M6	0.018(1)	0.021(1)	0.016(1)	−0.002(1)
M7	0.018(2)	0.022(2)	0.011(2)	0.001(1)
M8	0.036(2)	0.027(2)	0.021(2)	−0.007(1)
M9	0.031(2)	0.026(1)	0.021(2)	0.008(1)
M10	0.022(1)	0.023(1)	0.014(2)	−0.003(1)
M11	0.020(2)	0.020(1)	0.015(2)	0.000(1)
M12	0.015(2)	0.020(2)	0.015(2)	−0.001(1)
M13	0.022(1)	0.040(2)	0.030(2)	0.004(1)
M14	0.017(2)	0.019(2)	0.016(2)	0.000(1)
M15	0.030(1)	0.027(1)	0.021(1)	−0.004(1)
M16	0.029(1)	0.022(1)	0.017(1)	0.000(1)
M17	0.039(2)	0.028(2)	0.020(2)	0.005(1)
M18	0.023(2)	0.021(2)	0.012(1)	−0.002(1)
M19	0.019(1)	0.022(1)	0.013(1)	0.001(1)
M20	0.007(2)	0.042(3)	0.026(3)	0.002(2)
M21	0.025(2)	0.034(3)	0.024(3)	−0.001(1)
M22	0.025(1)	0.041(2)	0.023(2)	0.004(1)
M23	0.020(2)	0.022(2)	0.016(2)	0.000(1)
M24	0.030(7)	0.022(7)	0.019(7)	0.017(4)

Note: Standard deviations are in parentheses. The thermal parameters are of the form

$$\exp[-2\pi^2(U_{11}h^2a^{*2} + U_{22}k^2b^{*2} + U_{33}l^2c^{*2} + 2U_{12}hka^*b^* + 2U_{13}hla^*c^* + 2U_{23}klb^*c^*)].$$

TABLE 5. Interatomic distances (max.: 3.80 Å) in Bi-rich izoklakeite

M(1)–S(26)		2.807(20)	M(2)–S(3)		2.622(15)
–S(6)	2×	2.868(13)	–S(7)	2×	2.854(12)
–S(1)	2×	2.932(2)	–S(2)	2×	2.869(13)
–S(2)		3.081(19)	–S(6)		3.209(18)
M(3)–S(3)	2×	2.955(11)	M(4)–S(9)		2.497(17)
–S(7)		2.976(18)	–S(4)	2×	2.670(12)
–S(8)	2×	2.991(12)	–S(5)	2×	3.036(15)
–S(4)		3.155(19)	–M(21)		3.719(5)
–S(29)		3.268(16)	–M(20)		3.722(6)
M(5)–S(10)		2.610(17)	M(6)–S(11)		2.852(18)
–S(5)	2×	2.831(14)	–S(12)	2×	2.858(12)
–S(27)	2×	3.013(15)	–S(6)	2×	3.015(13)
–M(20)		3.521(7)	–S(7)		3.254(18)
–S(27)	2×	3.620(15)			
–M(5)		3.671(7)			
M(7)–S(8)		2.588(16)	M(8)–S(8)	2×	2.964(12)
–S(13)	2×	2.719(13)	–S(4)		3.009(18)
–S(7)	2×	3.022(13)	–S(9)	2×	3.117(14)
–S(12)		3.286(17)	–S(14)	2×	3.166(12)
			–S(13)		3.393(20)
M(9)–S(5)		2.988(19)	M(10)–S(12)		2.861(17)
–S(9)	2×	3.013(13)	–S(17)	2×	2.889(12)
–S(10)	2×	3.024(13)	–S(11)	2×	3.012(13)
–S(15)	2×	3.139(12)	–S(16)		3.131(20)
–S(16)		3.718(20)			
M(11)–S(17)		2.579(17)	M(12)–S(14)		2.555(16)
–S(18)	2×	2.679(10)	–S(19)	2×	2.653(12)
–S(12)	2×	3.024(12)	–S(13)	2×	3.049(14)
–S(13)		3.297(19)	–S(18)		3.184(16)
M(13)–S(15)	2×	3.000(12)	M(14)–S(15)		2.537(16)
–S(14)	2×	3.005(12)	–S(16)	2×	2.712(13)
–S(20)	2×	3.118(12)	–S(21)	2×	3.014(13)
–M(24)		3.324(11)	–S(11)		3.354(18)
–S(21)		3.420(18)			
–S(19)		3.572(20)			
M(15)–S(27)		2.711(17)	M(16)–S(23)	2×	2.915(12)
–S(10)	2×	2.878(13)	–S(22)	2×	3.046(12)
–S(22)	2×	2.911(12)	–S(18)		3.060(16)
–S(16)		3.019(19)	–S(28)		3.073(20)
			–S(17)	2×	3.302(13)
M(17)–S(24)	2×	2.814(11)	M(18)–S(20)		2.576(17)
–S(29)		2.947(16)	–S(21)	2×	2.810(12)
–S(23)	2×	3.035(13)	–S(25)	2×	2.836(13)
–S(18)		3.305(16)	–S(26)		3.139(20)
–S(19)	2×	3.495(15)			
–M(24)	2×	3.727(9)			
M(19)–S(11)	2×	2.867(12)	M(20)–S(22)		2.475(16)
–S(6)		2.907(18)	–S(28)	2×	2.758(14)
–S(26)	2×	2.993(14)	–S(27)	2×	2.960(15)
–S(21)		3.074(18)	–M(5)		3.521(7)
			–M(4)		3.722(6)
			–S(5)	2×	3.781(16)
M(21)–S(23)		2.551(17)	M(22)–S(24)	2×	2.972(12)
–S(29)	2×	2.678(11)	–S(3)	2×	2.988(11)
–S(28)	2×	3.081(15)	–S(25)	2×	3.125(15)
–M(4)		3.718(5)	–S(2)		3.272(19)
–S(4)	2×	3.760(15)	–S(29)		3.450(17)
M(23)–S(25)		2.653(19)	M(24)–S(24)		2.286(19)
–S(26)	2×	2.909(14)	–S(20)	2×	2.344(10)
–S(1)		2.950(3)	–S(19)		2.371(22)
–S(2)	2×	2.958(13)	–S(25)		3.216(22)
			–M(13)		3.324(11)
			–M(17)	2×	3.726(9)

10% of the actual temperature factor (Table 4). Displacement vectors (temperature factors) are still not sufficiently defined to interpret (Sb,Bi,Pb) ordering on the basis of difference vibrational parameters along the bonding vector (Chandrasekhar and Bürgi, 1984). Nevertheless, M(5) and M(20) show highly anisotropic displacement vectors so that disorder seems probable for these positions. Differences in bond lengths (Table 5) and in (Sb,Bi,Pb) distributions between the two structure refinements will be discussed in a later section.

Site-population refinements also indicate that the position M(24) is occupied by Cu and Fe but not by Ag. Thus Ag may partially replace Pb. If Ag is not statistically distributed over several positions but is concentrated on only a few sites, it may be mistaken for Sb. Makovicky and Mumme (1979) found (Bi,Ag) sites in benjaminite and Makovicky and Mumme (1983) described mixed (Sb,Ag) sites in ramdohrite. In 11 of the 23 available metal positions, partial occupation of light elements (probably Sb) could be identified by site-occupancy refinements. If we assume that Sb exclusively shares M sites with Bi because of its similar charge and size, then a surplus of Bi would be calculated, as compared to the analyzed concentration. Consequently, two alternative interpretations must be considered: (a) not all the alleged Sb is really Sb but some is actually Ag or (b) Sb also shares positions with Pb.

Characteristic coordination and Me-S (Me = Sb,Bi,Pb,Tl) distances in sulfides and sulfosalts

Sulfosalt structures may simultaneously contain Bi^{3+}, Pb^{2+}, and Tl^{+} or combinations of two of these elements, which cannot be distinguished by their scattering behavior of X-rays because they are isoelectronic (80 electrons). In addition, Sb^{3+} (48 electrons) may replace Bi^{3+}, whereas Ag^{+} (46 electrons) may substitute for Pb^{2+}. Additional

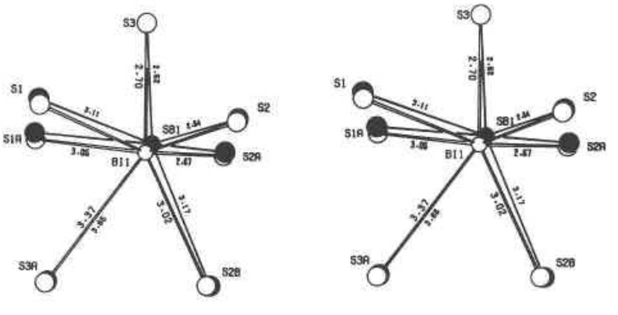

Fig. 2. Stereo plot of sevenfold-coordinated Sb(1) (filled circles) in Sb_2S_3 (Bayliss and Nowacki, 1972), and Bi(1) (open circles) in Bi_2S_3 (Kupčik and Veselá-Nováková, 1970). Sb(1) and Bi(1) coordination polyhedra are drawn above each other. Characteristic of SbS_n and BiS_n coordination are three short Me–S bonds and two to four longer ones. Responsible for the distorted coordination are lone electron pairs that point in the direction of the longer Me–S distances. The major difference between SbS_7 and BiS_7 in these structures is a stronger displacement of Sb out of the center of the S_7 environment, probably owing to the stronger influence of the lone electron pair in Sb^{3+}. The S arrangement, however, is very similar. The labels for Bi–S distances are larger than those for Sb–S distances. S(1) and S(1A) as well as S(2) and S(2A) are symmetry-equivalent sites.

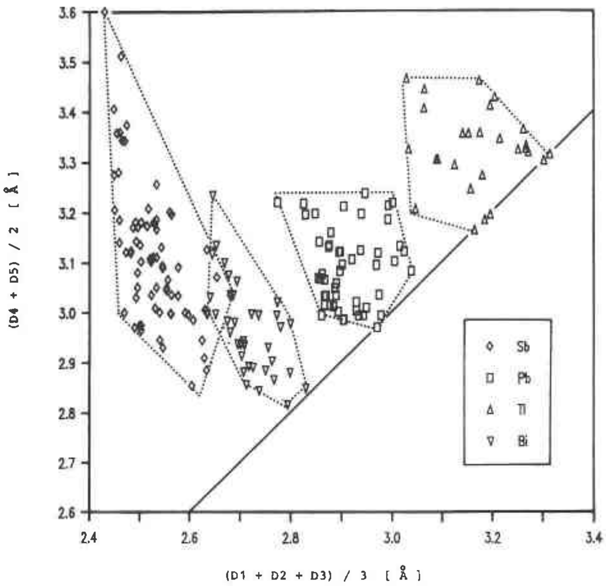

Fig. 3. The mean value of the three shortest Me–S distances is plotted against the mean value of the next two shortest ones. All data are obtained from published structures (Table 6). The structures considered were (1) those that contain only Bi, Pb, or Tl but not combinations of them and (2) those that contain Sb but do not bear significant Bi concentrations. These selection criteria became necessary to avoid ambiguous assignments. In addition, Me positions with short Me-Me distances were also excluded (see text). The plot displays coherent fields for element-specific Me–S distance distributions, which show more or less continuous transitions into the neighboring fields. Dotted lines confine the various distribution clouds. The solid line indicates undistorted coordination where (D1 + D2 + D3)/3 = (D4 + D5)/2.

criteria other than X-ray scattering behavior are therefore needed to differentiate between these atoms. Sb^{3+} and Bi^{3+} often reveal highly distorted coordination polyhedra (Fig. 2) owing to the strong influence of the lone electron pair on the stereochemistry of these elements (Olivier-Fourcade et al., 1978; Kupčik, 1972). This effect is less pronounced in the case of Pb^{2+} and Tl^{+}. The striking appearance of three short Me–S distances (Me = As,Sb,Bi) induced Nowacki (1969) to described the topology of sulfosalts by trigonal AsS_3, SbS_3, and BiS_3 pyramids.

In the past, most authors decided upon the (Bi,Pb) assignment on the basis of individual criteria (Kupčik, 1984: "crystal chemical experience") or by analogy with other related structures. Berry (1965) gave characteristic Me–S bond lengths for sulfosalts and distinguished three groups to bypass the problem of irregular coordination polyhedra: the shortest Me–S distance, the next two shortest, and the fourth and fifth distances. Unfortunately, only very few sulfosalts containing Bi or Tl were known at that time, and the quality of the available structure refinements was not as high as now. Shannon (1981), who tabulated bond distances in sulfides and "sulfide crystal radii" stated, "Sulfosalts of As, Sb, and Bi with irregular coordination and consequent increased bond distances have not been very useful in obtaining characteristic mean metal–sulphur distances . . . ," and consequently he avoided these structures.

We have constructed a simple diagram (Fig. 3) where the mean value of the three shortest Me–S (Me = Sb,Bi,Pb,Tl) distances [$x = (D1 + D2 + D3)/3$] is plotted against the mean value of the next two shortest ones [$y = (D4 + D5)/2$]. This diagram was obtained from structures stored in the inorganic crystal-structure database (Bergerhoff et al., 1983)[2] and additional papers. Sulfosalt and sulfide structures that contained only Bi or Pb or Tl were selected, thus eliminating the possibility of a wrong assignment. Because of the apparent difference in the number of electrons between Sb on the one hand and Bi,Pb, and Tl on the other, a special selection criterion seemed unnecessary for Sb-bearing sulfosalts. Bi^{3+} tends to substitute for Sb^{3+}, however, so Sb-bearing structures with additional Bi were also excluded. In addition, atomic positions with disorder problems, partial occupation, and Me-Me interactions were rejected. For Me-Me interactions, we defined Me-Me distances that were smaller than the 6 (or 5 for fivefold coordination) smallest Me–S distances. Positions that contained fourfold-coordinated Sb (mostly Sb^{5+}) were also excluded. Results for 21 structures with Tl (27 Tl positions), 20 structures with Pb (50 Pb positions), 16 structures with Bi (37 Bi positions), and 22 structures with Sb (72 Sb positions) are included in Figure 3. Table 6 summarizes chemical composition and

---

[2] To exclude errors from the inorganic crystal-structure database, most bond distances were checked with the original literature.

TABLE 6. Crystal structures selected for the bond-lengths diagram (Fig. 3)

Sb_2S_3	stibnite	Bayliss and Nowacki, 1972
$CuSbS_2$	wolfsbergite	Hofmann, 1933
$FeSb_2S_4$	berthierite	Buerger and Hahn, 1950
$AgSbS_2$	miargyrite	Knowles, 1964
$HgSb_4S_8$	livingstonite	Srikrishnan and Nowacki, 1975
$NaSbS_2$		Olivier-Fourcade et al., 1978
$NaSbS_2$		Kanishcheva et al., 1979
$Pb_3Sb_8S_{15}$	fülöppite	Nuffield, 1975
$Pb_3Sb_8Si_5$	fülöppite	Edenharter and Nowacki, 1974
$Pb_5Sb_8Si_7$	plagionite	Cho and Wuensch, 1970
$Pb_4Sb_4S_{11}$		Petrova et al., 1979
$Pb_6Sb_{14}S_{27}$	zinckenite	Portheine and Nowacki, 1975
$PbAgSbS_3$	freieslebenite	Ito and Nowacki, 1974a
$Pb_6Sb_{11}Ag_3S_{24}$	ramdohrite	Makovicky and Mumme, 1983
$TlSb_3S_5$		Gostojić et al., 1982
$TlSbS_2$	weissbergite	Rey et al., 1983
Tl_3SbS_3		Rey et al., 1984
$Tl_2(SbAs)_{10}S_{16}$	pierrotite	Engel et al., 1983
$Tl_8Pb_4Sb_{21}As_{19}S_{68}$		Nagl, 1979
$Rb_2Sb_4S_7$		Dittmar and Schäfer, 1978
$Cs_2Sb_8S_{13}$		Volk and Schäfer, 1979
$K_2Sb_4S_7$		Graf and Schäfer, 1972
Bi_2S_3	bismuthinite	Kupčik and Veselá-Nováková, 1970
$HgBi_2S_4$		Mumme and Watts, 1980
$RbBi_3S_5$		Schmitz and Bronger, 1974
$AgBi_3S_5$	pavonite	Makovicky et al., 1977
$CuBi_5S_8$		Ohmasa and Nowacki, 1973
$Cu_4Bi_4S_9$		Bente and Kupčik, 1984
$Cu_4Bi_5S_{10}$		Mariolacos et al., 1975
$Cu_{3.21}Bi_{4.79}S_9$		Ohmasa, 1973
$Bi_2In_4S_9$		Chapuis et al., 1972
$Bi_3In_5S_{12}$		Krämer, 1980
Eu_2BiS_4		Lemoine et al., 1982
$Eu_{1.1}Bi_2S_4$		Lemoine et al., 1986
$BiPS_4$		Zimmermann et al., 1975
$Bi_{3.78}Ce_{1.25}S_8$		Céolin et al., 1977
$Bi(Bi_2S_3)_9I_3$		Miehe and Kupčik, 1971
$Bi(Bi_2S_3)_9Br_3$		Mariolacos, 1976
PbS	galena	rock salt structure
$Pb_3Sb_8S_{15}$	fülöppite	Edenharter and Nowacki, 1974
$Pb_3Sb_8S_{15}$	fülöppite	Nuffield, 1975
$Pb_3Sb_8S_{17}$	plagionite	Cho and Wuensch, 1970
$Pb_4Sb_4S_{11}$		Petrova et al., 1979
$Pb_{28}As_{12}S_{46}$	jordanite	Ito and Nowacki, 1974b
$Pb_{12}As_{16}S_{36}$	baumhauerite	Engel and Nowacki, 1969
$PbCuAsS_3$	seligmannite	Takéuchi and Haga, 1969
$PbAgSbS_3$	freieslebenite	Ito and Nowacki, 1974a
$Pb_6Sb_{11}Ag_3S_{24}$	ramdohrite	Makovicky and Mumme, 1983
$Pb_{0.46}Mo_3S_4$		Guillevic et al., 1976
$Pb_{0.92}Mo_6S_{7.5}$		Marezio et al., 1973
$Pb_4In_9S_{17}$		Ginderow, 1978
$Pb_3In_{6.6}S_{13}$		Ginderow, 1978
$PbGeS_3$		Ribes et al., 1974
$GePb_2S_4$		Susa and Steinfink, 1971
$SiPb_2S_4$		Iglesias and Steinfink, 1973
$PbSnS_3$		Jumas et al., 1972
$Pb_2Ga_2S_5$		Mazurier et al., 1980
$PbZrS_2$		Lelieveld and Ijdo, 1978
Tl_2S_5		Leclerc and Kabré, 1975
$TlSb_3S_5$		Gostojić et al., 1982
Tl_3SbS_4		Gostojić et al., 1981
$TlSb_5S_8$	parapierrotite	Engel, 1980
$TlSbS_2$	weissbergite	Rey et al., 1983
Tl_3SbS_3		Rey et al., 1984
$Tl_2(Sb,As)_{10}S_{16}$	pierrotite	Engel et al., 1983
Tl_3AsS_4		Engel and Nowacki, 1984
Tl_3AsS_3	ellisite	Gostojić, 1980
$Tl_5Sb_5As_8S_{22}$	rebulite	Balić-Žunić et al., 1982
$TlFeS_2$		Kutoglu, 1974
$TlErS_2$		Kabré et al., 1974
$TlCoS_2$		Klepp and Boller, 1978
$TlInS_2$-II		Range et al., 1974
$TlInS_2$-III		Range et al., 1974
Tl_3VS_4		Vlasse and Fournes, 1978
$TlCu_3S_2$		Klepp and Yvon, 1980
$Tl_4Ge_2S_6$		Eulenberger, 1978
$Tl_4(Mo_6S_8)(Mo_{12}S_{14})$		Potel et al., 1980
$Tl_2MnAs_2S_5$		Gostojić et al., 1982
$Hg_3Tl_4As_4Sb_2S_{20}$	vrbaite	Ohmasa and Nowacki, 1971

references for the structures studied. It must be noted that vacancies or substitutions of low concentrations (<10%) of other ions on these positions do not exert significant influence because of the low accuracy of most Me–S distances.

Figure 3 displays a coherent field for each element. However, the fields merge almost continuously with each other, especially in the case of Sb and Bi. As expected, Tl and Pb possess rather regular Me–S distances. The influence of the lone electron pair becomes striking for Bi and, especially, Sb, leading to strongly elongated fields in Figure 3. Nevertheless, there are also regular BiS_6 octahedra [e.g., $CuBi_5S_8$ (Ohmasa and Nowacki, 1973)] and one regular SbS_6 octahedron is known in β-$NaSbS_2$, which crystallizes in the NaCl-type structure with Na and Sb occupying octahedral positions (Olivier-Fourcade et al., 1978).

The statistically decreasing influence of the lone electron pair on the distortion of the Me coordination polyhedra from Sb to Tl may be explained by the increasing size of the ion ($Sb^{3+} < Bi^{3+} < Pb^{2+} < Tl^{+}$). For atoms with a large surface, the S atoms can be distributed without interfering with the lone electron pair; thus the surrounding S atoms show more even distances to the central atom (e.g., Pb^{2+}, Tl^{+}). For atoms with a smaller diameter and thus a smaller surface (Sb^{3+}, Bi^{3+}), the orientation of the lone electron pair disturbs a regular coordination, which is reflected in three short Me–S distances and two to five longer Me–S distances.

(Bi,Pb) ordering in sulfosalts

Several structures are known to contain combinations of Bi and Pb but no Sb. Some examples were selected to compare the (Bi,Pb) distribution proposed in the original structural study with a distribution suggested by our model (Fig. 3). A well-ordered (Bi,Pb) distribution was suggested in the original literature for the structures of $Cu_3Pb_3Bi_7S_{15}$, lindströmite (Horiuchi and Wuensch, 1976); $CuPbBi_3S_6$, krupkaite (Mumme, 1975); $Pb_2Bi_2S_5$, cosalite (Srikrishnan and Nowacki, 1974); $PbBi_2S_4$, galenobismutite (Iitaka and Nowacki, 1962), $Cu_2Pb_2Bi_4S_9$, hammarite (Horiuchi and Wuensch, 1977); $CuPbBiS_3$, aikinite (Ohmasa and Nowacki, 1970), and synthetic $Pb_{1.6}In_8Bi_4S_{19}$ (Krämer, 1983). For $Pb_3Bi_2S_6$, lillianite (Takagi and Takéuchi, 1972) and $CuPb_2(Pb,Bi)Bi_2S_7$, nuffieldite (Kohatsu and Wuensch, 1973), positions with mixed (Bi,Pb) occupation were assumed. In eclarite, $(Cu,Fe)Pb_9Bi_{12}S_{28}$ (Kupčik, 1984), eight Me positions were assigned to Bi, an additional eight positions were assigned to Pb, and five positions were not specified. The characteristic $x = (D1 + D2 + D3)/3$ and $y = (D4 + D5)/2$ bond distances for these examples were plotted against each other in Figure 4. The (Bi,Pb) assignment chosen by the original authors agrees for most structures with our model (most points plot in the corresponding field). Some discrepancies are observed for cosalite, nuffieldite, hammarite, and synthetic $Pb_{1.6}In_8Bi_4S_{19}$. Few atomic sites assigned to Pb plot within our Bi field, and several positions situated in the transition zone between the Pb and Bi field were attributed to either one of the elements, although partial (Bi,Pb) occupation cannot be ruled out according to Figure 4. For lillianite a statistical distribution of Bi and Pb was assumed (Takagi and Takéuchi, 1972). However, Figure 4 suggests that the M(3) site is enriched in Pb, whereas M(1) and M(2) are preferentially occupied by Bi.

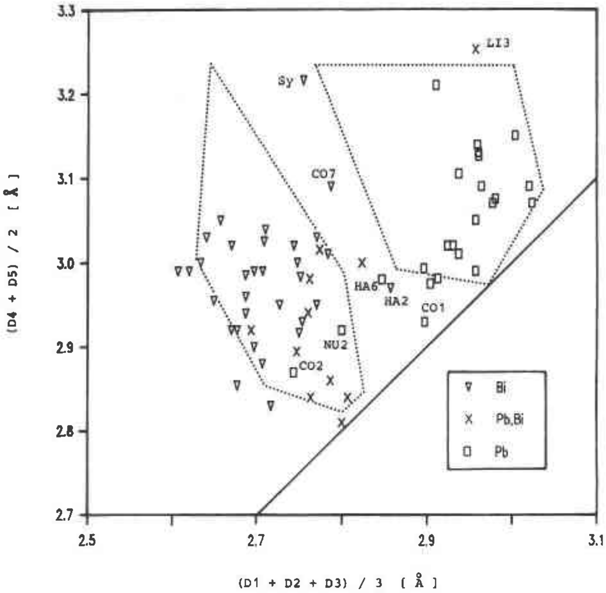

Fig. 4. The mean value of the three shortest Me–S distances is plotted against the mean value of the next two shortest ones as in Figure 3. The fields confined by dotted lines are also adopted from Figure 3 and represent (from left to right) fields characteristic of Bi–S and Pb–S distance distributions. Only structures of (Pb,Bi) sulfosalts are considered. The symbols for mixed or undecided occupation (× symbols), Pb (squares), or Bi sites (triangles) represent Me (Pb, Bi) assignments chosen by the authors of the various structure refinements. The plot tests whether a selected Me assignment is in agreement with the distribution clouds defined in Figure 3 (see text). Some questionable assignments were detected for cosalite (CO), hammarite (HA), nuffieldite (NU), lillianite (LI), and synthetic $Pb_{1.6}In_8Bi_4S_{19}$ (SY).

(Pb,Bi,Sb) ordering in izoklakeite

The element-specific fields defined in Figure 3 were also used to estimate the metal distribution in izoklakeite. Characteristic Me–S distance $(D1 + D2 + D3)/3$ vs. $(D4 + D5)/2$ are plotted (Fig. 5) for the Bi-rich Zervreila izoklakeite (this paper) and the Sb-rich Vena izoklakeite of Makovicky and Mumme (1986).

For the Zervreila izoklakeite, 10 Me sites [M(3), M(6), M(8), M(9), M(10), M(13), M(16), M(17), M(19), M(22)] plot within the Pb field. However, 13.4 Pb atoms are available per asymmetric unit. No Sb or Ag has been found in site-occupancy refinements for these 10 positions. Three additional positions [M(1), M(15), M(23)] lie between the Bi field and the Pb field (or on the upper boundary of the Bi field). M(1) and M(15) are considered to be mixed (Pb,Bi) sites, whereas 0.23 Sb (or Ag) was

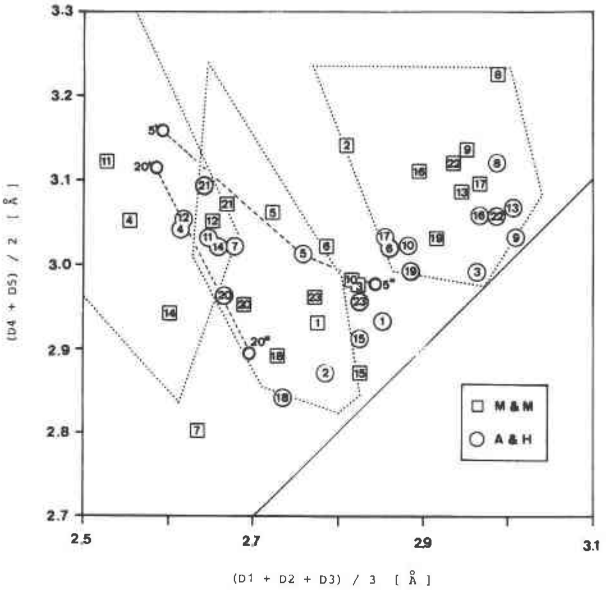

Fig. 5. In order to find appropriate Sb, Bi, and Pb assignments for izoklakeites [this paper: circles; values from Makovicky and Mumme (1986): squares], the mean value of the three shortest Me–S distances is plotted vs. the next two shortest ones. The fields confined by dotted lines are adopted from Fig. 3 and represent (from left to right) fields characteristic of Sb–S, Bi–S, and Pb–S distance distributions. If M(5) and M(20) are interpreted as disordered split positions (displaced ±0.2 Å from M(5) and M(20) along the longest axis of the displacement ellipsoid), the atomic sites connected by dashed lines [M(5′), M(5″), and M(20′), M(20″)] result.

refined for M(23); thus M(23) is a mixed [Sb(Ag),Bi,Pb] position. For all remaining sites [M(2), M(4), M(5), M(7), M(11), M(12), M(14), M(18), M(20), M(21)] that plot within the Sb or Bi field or in the overlap region between these two fields, various concentrations of Sb (or Ag) have been identified in site-occupancy refinements. M(20) is a pure Sb position. Not all available Pb could be distributed over Pb and mixed (Pb,Bi) positions; thus it must be assumed that the remaining sites contain Bi and Sb with additional low Pb concentrations.

As already mentioned above, M(5) exhibits a highly anisotropic displacement parameter (temperature factor) with the longest axis of the ellipsoid pointing parallel to ⟨110⟩. On the other hand, M(5) is one of the most Sb-rich positions (0.37 Sb), but plots in the center of the Bi field (Fig. 5) and displays longer Me–S distances than other Sb-enriched positions. These observations lead to the interpretation of M(5) as a split position. If two sites are created by shifting the atom position (±0.2 Å) along the longest axis of the displacement ellipsoid, one resulting M(5) site [M(5′)] moves towards the Sb field (Fig. 5), whereas the other M(5) site [M(5″)] shifts into the (Bi,Pb) intermediate area. If corresponding Sb and Bi positions are compared in the isotypic structures of bismuthinite (Kupčik and Veselá-Nováková, 1970) and stibnite (Bayliss and Nowacki, 1972, it can be seen (Fig. 2) that the arrangement of coordinating S atoms is very similar, whereas Sb and Bi are displaced against each other. This example indicates that mixed (Sb,Bi) positions will reflect increased displacement parameters, as observed in M(5).

M(20), the pure Sb site, which is connected with M(5) by S(27), also displays a highly anisotropic displacement ellipsoid with the longest axis parallel to **b.** In Figure 5,

TABLE 7. Cation assignments in izoklakeites

Site	Zervreila (this paper)	Vena* (this paper)	Vena (Makovicky and Mumme, 1986)
M1	Bi,Pb	Bi,Pb	0.80Pb + 0.20Bi
M2	0.10(4)Sb + 0.90(**Bi**,Pb)	Pb	0.60Pb + 0.40Bi
M3	Pb	Bi,Pb	0.80Pb + 0.20Bi
M4	0.45(4)Sb + 0.55(**Bi**,Pb)	0.65Sb + (**Bi**,Pb)	0.65Sb + 0.35Bi
M5	0.37(6)Sb + 0.63(**Bi**,Pb)	0.85Sb + (**Bi**,Pb)	0.85Sb + 0.15Bi
M6	Pb	Bi,Pb	Pb
M7	0.22(4)Sb + 0.78(**Bi**,Pb)	0.40Sb + 0.60(**Bi**,Pb)	0.40Sb + 0.60Bi
M8	Pb	Pb	Pb
M9	Pb	Pb	Pb
M10	Pb	Bi,Pb	Pb
M11	0.05(3)Sb + 0.95(**Bi**,Pb)	0.40Sb + 0.60(**Bi**,Pb)	0.40Sb + 0.60Bi
M12	0.27(4)Sb + 0.73(**Bi**,Pb)	0.40Sb + 0.60(**Bi**,Pb)	0.40Sb + 0.60Bi
M13	Pb	Pb	Pb
M14	0.23(4)Sb + 0.77(**Bi**,Pb)	0.55Sb + 0.45(**Bi**,Pb)	0.55Sb + 0.45Bi
M15	Bi,Pb	Bi,Pb	Pb
M16	Pb	Pb	Pb
M17	Pb	Pb	Pb
M18	0.09(4)Sb + 0.91(**Bi**,Pb)	0.45Sb + 0.55(**Bi**,Pb)	0.45Sb + 0.55Bi
M19	Pb	Pb	Pb
M20	SB	Sb	Sb
M21	0.38(5)Sb + 0.62(**Bi**,Pb)	0.60Sb + 0.40(**Bi**,Pb)	0.60Sb + 0.40Bi
M22	Pb	Pb	Pb
M23	0.23(4)Sb + 0.77(**Bi**,Pb)	**Bi**,Pb	0.60Bi + 0.40Pb

* Sb assignment is taken from Makovicky and Mumme (1986).

M(20) plots on the boundary between the Sb and the Bi field. The elongated displacement ellipsoid may also be interpreted as a split Sb position. M(20′) and M(20″) are created by shifting M(20) ± 0.2 Å along **b.** M(20′) plots within the Sb field; however, M(20″) remains on the borderline of the Bi field. For M(20′) the three shortest Me–S distances are formed by S(22) and 2 × S(28), whereas S(22) and 2 × S(27) form the three shortest Me–S distances for M(20″). Thus M(20) could be interpreted as a hybrid between M(20′), type 3 + 2 (Me–S: 2.49, 2.63, 2.63; 3.11, 3.11) and M(20″) type 1 + 4 (Me–S: 2.47; 2.82, 2.82, 2.89, 2.89) as discussed by Kupčik (1972). Because of the small separation of the split positions, no attempt has been made to refine such atomic sites.

Out of 12.8 available Pb atoms per asymmetric unit for the Vena izoklakeite (Makovicky and Mumme, 1986), eight sites [M(2), M(8), M(9), M(13), M(16), M(17), M(19), M(22)] plot within the Pb field. Four additional positions [M(3), M(6), M(10), M(15)] lie in the intermediate area between the Pb and Bi field (or on the boundary of the Bi field); thus a mixed (Pb,Bi) occupation must be suggested. Makovicky and Mumme (1986) did not consider light elements for M(1) and M(23), which both plot within the Bi field. However, there is still a surplus of Pb; thus mixed (Bi,Pb) occupation is also assumed for M(1) and M(23). All remaining sites carry variable amount of Sb. As observed in the Zervreila izoklakeite, M(20) is a pure Sb site. Table 7 compares the cation assignment of the Bi-rich Zervreila izoklakeite with the cation assignment of the Sb-rich crystal of Makovicky and Mumme (1986) (1) by the method proposed in this paper and (2) by semiquantitative values given by Makovicky and Mumme (1986).

Besides izoklakeite there are only very few well-refined sulfosalt structures that contain Sb and Bi or even Sb, Bi, and Pb in significant amounts: jaskolskiite, Cu_x-$Pb_{2+x}(Sb,Bi)_{2-x}S_5$ ($x = 0.2$) (Makovicky and Nørrestam, 1985); kobellite, $(Cu_{0.56}Fe_{0.44})_2Pb_{12}(Bi_{0.56}Sb_{0.44})S_{14}$, (Miehe, 1971); and aramayoite, $Ag(Sb,Bi)S_2$ (Mullen and Nowacki, 1974). For most positions in these structures, a random (Sb,Bi) distribution was assumed.

ACKNOWLEDGMENTS

We are grateful to V. Kupčik (Göttingen, FRG), T. Balić-Žunič (Zagreb, Jugoslavia), A. Gutiérrez (Bern), and R. Welch (Bern) for reviewing the manuscript.

REFERENCES

Armbruster, Th., Stalder, H.A., and Oberhänsli, R. (1984) Antimonreicher Giessenit vom Zervreilasee (Vals, Graubünden). Schweizerische Mineralogische und Petrographische Mitteilungen, 64, 21–26.

Balić-Žunić, T., Šćavnićar, S., and Engel, P. (1982) The crystal structure of rebulite, $Tl_5Sb_5As_8S_{22}$. Zeitschrift für Kristallographie, 160, 109–125.

Bayliss, P., and Nowacki, W. (1972) Refinement of the crystal structure of stibnite Sb_2S_3. Zeitschrift für Kristallographie, 135, 308–315.

Bente, K., and Kupčik, V. (1984) Redetermination and refinement of the structure of tetrabismuth tetracopper enneasulphide, $Cu_4Bi_4S_9$. Acta Crystallographica, C40, 1985–1986.

Bergerhoff, G., Hundt, F., Sievers, R., and Brown, I.D. (1983) The inorganic crystal structure data base. Journal of Chemical Information and Computer Science, 23, 66–69.

Berry, L.G. (1965) Recent advances in sulfide mineralogy. American Mineralogist, 50, 301–313.

Buerger, M.J., and Hahn, T. (1950) The crystal structure of berthierite, $FeSb_2S_4$. American Mineralogist, 40, 226–238.

Céolin, R., Tooli, P., Khodadad, P., and Rodier, N. (1977) Structure cristalline du sulfure mixte de cerium et de bismuth $Ce_{1.25}Bi_{3.78}S_8$. Acta Crystallographica, B33, 2804–2806.

Chandrasekhar, K., and Bürgi, H.B. (1984) Dynamic processes in crystals examined through difference vibrational parameters U: The low-spin–high-spin transition in tris(dithiocarbamato)ironIII complexes. Acta Crystallographica, B40, 387–397.

Chapuis, G., Gnehm, Ch., and Kraemer, V. (1972) Crystal structure and crystal chemistry of bismuth indium sulfide, $Bi_2In_4S_9$. Acta Crystallographica, B28, 3128–3130.

Cho, S. A., and Wuensch, B. J. (1970) Crystal chemistry of the plagionite group. Nature, 225, 444–445.

Dittmar, G., and Schäfer, H. (1978) Darstellung und Kristallstruktur von $Rb_2Sb_4S_7$. Zeitschrift für allgemeine und anorganische Chemie, 441, 93–97.

Edenharter, A., and Nowacki, W. (1974) Die Kristallstruktur von Füllöppit, $Pb_3Sb_8S_{15}$. Neues Jahrbuch für Mineralogie Monatshefte, 1974, 92–94.

Engel, P. (1980) Die Kristallstruktur von Parapierrotit, $TlSb_5S_8$. Zeitschrift für Kristallographie, 151, 203–216.

Engel, P., and Nowacki, W. (1969) Die Kristallstruktur von Baumhauerit. Zeitschrift für Kristallographie, 129, 178–202.

——— (1984) Refinement of the crystal structure of synthetic Tl_3AsS_4. Croatica Chemica Acta, 57, 499–505.

Engel, P., Gostojić, M., and Nowacki, W. (1983) The crystal structure of pierrotite, $Tl_2(As,Sb)_{10}S_{16}$. Zeitschrift für Kristallographie 165, 209–215.

Enraf-Nonius. (1983) Structure determination package (SDP). Enraf-Nonius, Delft.

Eulenberger, G. (1978) Tetrathallium(I)-di-μ-tetrathio-digermanat. Acta Crystallographica, B34, 2614–2616.

Ginderow, D. (1978) Structures cristallines de $Pb_4In_9S_{17}$ et $Pb_3In_{6.67}S_{13}$. Acta Crystallographica, B34, 1804–1811.

Gostojić, M. (1980) Die Kristallstruktur von synthetischem Ellisit, Tl_3AsS_3. Zeitschrift für Kristallographie, 151, 249–254.

Gostojić, M., Nowacki, W., and Engel, P. (1981) The crystal structure of synthetic Tl_3SbS_4. Zeitschrift für Kristallographie, 157, 299–308.

——— (1982) The crystal structure of synthetic $TlSb_3S_5$. Zeitschrift für Kristallographie, 159, 217–224.

Gostojić, M., Edenharter, A., Nowacki, W., and Engel, P. (1982) The crystal structure of synthetic $Tl_2MnAs_2S_5$. Zeitschrift für Kristallographie, 158, 43–51.

Graeser, S. (1963) Giessenit- ein neues Pb-Bi-Sulfosalz aus dem Dolomit des Binnatales. Schweizerische Mineralogische und Petrographische Mitteilungen, 43, 471–478.

Graeser, S., and Harris, D.C. (1986) Giessenite from Giessen near Binn, Switzerland: New data. Canadian Mineralogist, 24, 19–20.

Graf, H.A., and Schäfer, H. (1972) Darstellung und Kristallstruktur des $K_2Sb_4S_7$. Zeitschrift für Naturforschung, Teil B, 27, 735–739.

Guillevic, J., Lestrat, H., and Grandjean, D. (1976) Etude structurale de combinaisons sulfurées et séléniées du molybdène. VI. Structures cristallines de $Pb_xMo_3S_4$ et de $Pb_xMo_3Se_4$. Acta Crystallographica, B32, 1342–1345.

Harris, D.C., Roberts, A.C., and Criddle, A.J. (1986) Izoklakeite, a new mineral species from Izok Lake, Northwest Territories. Canadian Mineralogist, 24, 1–5.

Hofmann, W. (1933) Strukturelle und morphologische Zusammenhänge bei Erzen vom Formeltypus ABC_2 I. Die Struktur von Wolfsbergit $CuSbS_2$ und Emplektit $CuBiS_2$, und deren Beziehung zu der Struktur von Antimonit Sb_2S_3. Zeitschrift für Kristallographie, 84, 177–203.

Horiuchi, H., and Wuensch, B.J. (1976) The ordering scheme for metal atoms in the crystal structure of hammarite, $Cu_2Pb_2Bi_4S_9$. Canadian Mineralogist, 14, 536–539.

——— (1977) Lindströmite, $Cu_3Pb_3Bi_7S_{15}$: Its space group and ordering scheme for metal atoms in the crystal structure. Canadian Mineralogist, 15, 527–539.

Iglesias, J.E., and Steinfink, H. (1973) Ternary chalcogenide compounds AB_2X_4. The crystal structures of $SiPb_2S_4$ and $SiPb_2Se_4$. Journal of Solid State Chemistry, 6, 93–98.

Iitaka, Y., and Nowacki, W. (1962) A redetermination of the crystal structure of galenobismutite, $PbBi_2S_4$. Acta Crystallographica, 15, 691–698.

Ito, T., and Nowacki, W. (1974a) The crystal structure of freieslebenite, $PbAgSbS_3$. Zeitschrift für Kristallographie, 139, 85–102.

——— (1974b) The crystal structure of jordanite, $Pb_{28}As_{12}S_{46}$. Zeitschrift für Kristallographie, 139, 161–185.

Jumas, J.C., Ribes, M., Philippot, E., and Maurin, M. (1972) Sur le systeme SnS_2-PbS. Structure cristalline de $PbSnS_3$. Comptes Rendus, Serie C 275, 269–272.

Kabré, S., Julien-Pouzol, M., and Guittard, M. (1974) Etude cristallographique des combinaisons ternaires formées par le thallium, les terres rares et le souffre, les selenium ou le tellure, le long des binaires Tl_2X-L_2X_3. Bulletin de la Société Chimique de France, 9, 1881–1884.

Kanishcheva, A.S., Kuznetsov, V.G., and Batog, V.N. (1979) Crystal structure of α-$NaSbS_2$. Zhurnal Strukturnoi Khimii, 20, 148–152.

Karup-Møller, S. (1973) A Giessenite-cosalite-galena–bearing mineral suite from Bjorkåsen sulphide deposit at Otoften in northern Norway. Norsk Geologisk Tidsskrift, 53, 41–64.

Klepp, K., and Boller, H. (1978) Ternäre Thallium-Uebergangsmetall-Chalkogenide mit $ThCr_2Si_2$ Struktur. Monatshefte für Chemie und verwandte Teile anderer Wissenschaften, 109, 1049–1057.

Klepp, K., and Yvon, K. (1980) Thallium dithiotricuprate(I). Acta Crystallographica, B36, 2389–2391.

Knowles, C.R. (1964) A redetermination of the structure of miargyrite, $AgSbS_2$. Acta Crystallographica, 17, 847–851.

Kohatsu, I., and Wuensch, B.J. (1973) The crystal structure of nuffieldite, $Pb_2Cu(Pb,Bi)Bi_2S_7$. Zeitschrift für Kristallographie, 138, 343–365.

Krämer, V. (1980) Structure of bismuth indium sulphide, $Bi_3In_5S_{12}$. Acta Crystallographica, B36, 1922–1923.

——— (1983) Lead indium bismuth chalcogenides. I. Structure of $Pb_{1.6}In_8Bi_4S_{19}$. Acta Crystallographica, C39, 1328–1329.

Kupčik, V. (1972) Bismuth. In K.H. Wedepohl, Ed., Handbook of geochemistry, vol. II/3, 83A, 1–7. Springer-Verlag, Berlin.

——— (1984) Die Kristallstruktur des Minerals Eclarit. $(Cu,Fe)Pb_9Bi_{12}S_{28}$. Tschermaks Mineralogische und Petrographische Mitteilungen, 32, 259–269.

Kupčik, V., and Veselá-Nováková, L. (1970) Zur Kristallstruktur des Bismuthinits, Bi_2S_3. Tschermaks Mineralogische und Petrographische Mitteilungen, 14, 55–59.

Kutoglu, A. (1974) Synthese und Kristallstrukturen von $TlFeS_2$ und $TlFeSe_2$. Naturwissenschaften, 61, 125–126.

Leclerc, B., and Kabré, T.S. (1975) Structure cristalline du sulfure de thallium, Tl_2S_5. Acta Crystallographica, B31, 1675–1677.

Lelieveld, R., and Ijdo, D.J.W. (1978) Lead zirconium sulfide. Acta Crystallographica, B34, 3348–3349.

Lemoine, P., Carré, D., and Guittard, M. (1982) Structure cristalline du sulfure d'europium et de bismuth Eu_2BiS_4. Acta Crystallographica, B38, 727–729.

——— (1986) Structure du sulfure d'europium et de bismuth $Eu_{1.1}Bi_2S_4$. Acta Crystallographica, C42, 259–261.

Main, P., Hull, S.E., Lessinger, L., Germain, G., Declercq, J.-P., and Woolfson, M.M. (1978) MULTAN78. A system of computer programs for the automatic solution of crystal structures from X-ray diffraction data. University of York, England and Louvain, Belgium.

Makovicky, E. (1981) The building principles and classification of bismuth-lead sulphosalts and related compounds. Fortschritte der Mineralogie, 59, 137–190.

——— (1985) The building principles and classification of sulphosalts based on the SnS archetype. Fortschritte der Mineralogie, 63, 45–89.

Makovicky, E., and Karup-Møller, S. (1986) New data on giessenite from the Bjørkåsen sulfide deposit at Otoften, northern Norway. Canadian Mineralogist, 24, 21–25.

Makovicky, E., and Mumme, W.G. (1979) The crystal structure of benjaminite $Cu_{0.50}Pb_{0.40}Ag_{2.30}Bi_{6.60}S_{12}$. Canadian Mineralogist, 17, 607–618.

——— (1983) The crystal structure of ramdohrite, $Pb_6Sb_{11}Ag_3S_{24}$, and its implications for the andorite group and zinckenite. Neues Jahrbuch für Mineralogie Abhandlungen, 147, 58–79.

——— (1984) The crystal structure of izoklakeite, dadsonite and jaskolskiite. Acta Crystallographica, A40, supplement, C-246.

——— (1986) The crystal structure of izoklakeite, $Pb_{51.3}Sb_{20.4}Bi_{19.5}Ag_{1.2}Cu_{2.9}Fe_{0.7}S_{114}$; The kobellite homologous series and its derivatives. Neues Jahrbuch für Mineralogie Abhandlungen, 153, 121–145.

Makovicky, E., and Nørrestam, R. (1985) The crystal structure of jaskolskiite, $Cu_xPb_{2+x}(Sb,Bi)_{2-x}S_5(x = 0.2)$, a member of the meneghinite homologous series. Zeitschrift für Kristallographie, 171, 179–194.

Makovicky, E., Mumme, W.G., and Watts, J.A. (1977) The crystal structure of synthetic pavonite, $AgBi_3S_5$, and the definition of the pavonite homologous series. Canadian Mineralogist, 15, 339–348.

Marezio, M., Dernier, P.D., Remeika, J.P., Corenzwit, E., and Matthias, B.T. (1973) Superconductivity of ternary sulfides and the structure of $PbMo_6S_8$. Material Research Bulletin 8, 657–668.

Mariolacos, K. (1976) The crystal structure of $Bi(Bi_2S_3)_9Br_3$. Acta Crystallographica, B32, 1947–1949.

Mariolacos, K., Kupčik, V., Ohmasa, M., and Miehe, G. (1975) The crystal structure of $Cu_4Bi_5S_{10}$ and its relation to the structures of hodrushite and cuprobismutite. Acta Crystallographica, B31, 703–708.

Mazurier, A., Jaulmes, S., and Guittard, M. (1980) Structure du pentasulfure de digallium et de diplomb. Acta Crystallographica, B 36, 1990–1993.

Miehe, G. (1971) Crystal structure of kobellite. Nature Physical Science, 231, 133–134.

Miehe, G., and Kupčik, V. (1971) Die Kristallstruktur des $Bi(Bi_2S_3)_9I_3$. Naturwissenschaften, 58, 219.

Mullen, D.J.E., and Nowacki, W. (1974) The crystal structure of aramayoite $Ag(Sb,Bi)S_2$. Zeitschrift für Kristallographie, 139, 54–69.

Mumme, W.G. (1975) The crystal structure of krupkaite, $CuPbBi_3S_6$ from the Juno Mine at Tennant Creek, Northern Territory, Australia. American Mineralogist, 60, 300–308.

Mumme, W.G., and Watts, J.A. (1980) $HgBi_2S_4$: Crystal structure and relationship with the pavonite homologous series. Acta Crystallographica, B36, 1300–1304.

Nagl, A. (1979) The crystal structure of a thallium sulfosalt, $Tl_8Pb_4Sb_{21}As_{19}S_{68}$. Zeitschrift für Kristallographie, 150, 85–106.

Nowacki, W. (1969) Zur Klassifikation und Kristallchemie der Sulfosalze. Schweizerische Mineralogische und Petrographische Mitteilungen, 49, 109–156.

Nuffield, E.W. (1975) The crystal structure of fülöppite, $Pb_3Sb_8S_{15}$. Acta Crystallographica, B31, 151–157.

Ohmasa, M. (1973) The crystal structure of $Cu_{2+x}Bi_{6-x}S_9$ ($x = 1.21$). Neues Jahrbuch für Mineralogie Monatshefte, 1973, 227–233.

Ohmasa, M.,. and Nowacki, W. (1970) A redetermination of the crystal structure of aikinite $[BiS_2/S/Cu^{IV}Pb^{VII}]$. Zeitschrift für Kristallographie, 132, 71–86.

——— (1971) The crystal structure of vrbaite, $Hg_3Tl_4As_8Sb_2S_{20}$. Zeitschrift für Kristallographie, 134, 360–380.

——— (1973) The crystal structure of synthetic $CuBi_5S_8$. Zeitschrift für Kristallographie, 137, 422–432.

Olivier-Fourcade, J., Philippot, E., and Maurin, M. (1978) Structure des composés $NaSbS_2\alpha$ et $NaSbS_2\beta$. Etude de l'influence de la paire electronique E de l'antimoine III dans la transition $NaSbS_2\alpha \rightarrow NaSbS_2\beta$. Zeitschrift für anorganische und allgemeine Chemie, 446, 159–168.

Petrova, I.V., Bortnikov, M.S., Pobedimskaya, E.A., and Belov, N.V. (1979) Crystal structure of a new synthetic lead-antimony sulfosalt. Doklady Akademii Nauk SSSR, 244, 607–609.

Portheine, J.C., and Nowacki, W. (1975) Refinement of the crystal structure of zinckenite, $Pb_6Sb_{14}S_{27}$. Zeitschrift für Kristallographie, 141, 79–96.

Potel, M., Chevrel, R., and Sergent, M. (1980) Structure de $Tl_2Mo_9S_{11}$, clusters Mo_{12} et Mo_6 isoles. Acta Crystallographica, B36, 1319–1322.

Range, K. J., Engert, G., Müller, W., and Weiss, A. (1974) Hochdrucksynthese und Kristallstrukturen von $TlInS_2$-II und $TlInS_2$-III. Zeitschrift für Naturforschung, Teil B, 29, 181–185.

Rey, N., Jumas, J.C., Olivier-Fourcade, J., and Philippot, E. (1983) Sur les composés III-V-VI: Etude structurale du disulfure d'antimoine et de thallium, $TlSbS_2$. Acta Crystallographica, C39, 971–974.

——— (1984) Structure du trisulfure d'antimoine et de trithallium, Tl_3SbS_3. Acta Crystallographica C40, 1655–1658.

Ribes, M., Olivier-Fourcade, J., Philippot, E., and Maurin, M. (1974) Structure cristalline d'un thiogermanate de plomb à chaines infinies $(PbGeS_3)_n$. Acta Crystallographica, B30, 1391–1395.

Schmitz, D., and Bronger, W. (1974) Die Kristallstruktur von $RbBi_3S_5$. Zeitschrift für Naturforschung, Teil B, 29, 438–439.

Schomaker, V., and Marsh, R.E. (1983) On evaluating the standard deviation of U_{eq}. Acta Crystallographica, A39, 819–820.

Shannon, R.D. (1981) Bond distances in sulfides and a preliminary table of sulfide crystal radii. In M. O'Keeffe and A. Navrotsky, Eds., Structure and bonding in crystals, vol. II, p. 53–70. Academic Press, New York.

Srikrishnan, T., and Nowacki, W. (1974) A redetermination of the crystal structure of cosalite, $Pb_2Bi_2S_5$. Zeitschrift für Kristallographie, 140, 114–136.

——— (1975) A redetermination of the crystal structure of livingstonite, $HgSb_4S_8$. Zeitschrift für Kristallographie, 141, 174–192.

Susa, K., and Steinfink, H. (1971) Ternary sulfide compounds AB_2S_4. The crystal structures of $GePb_2S_4$ and $SnBa_2S_4$. Journal of Solid State Chemistry, 3, 75–82.

Takagi, J., and Takéuchi, Y. (1972) The crystal structure of lillianite. Acta Crystallographica, B28, 649–651.

Takéuchi, Y., and Haga, N. (1969) On the crystal structure of seligmannite, $PbCuAsS_3$, and related minerals. Zeitschrift für Kristallographie, 130, 254–260.

Vlasse, M., and Fournes, L. (1978) Etude structurale de la phase Tl_3VS_4. Comptes Rendus, C-287, 47–49.

Volk, K., and Schäfer, H. (1979) $Cs_2Sb_8S_{13}$, ein neuer Formel- und Strukturtype bei Thioantimoniten. Zeitschrift Für Naturforschung, Teil B, 34, 1637–1640.

Zakrzewski, M.A., and Makovicky, E. (1986) Izoklakeite from Vena, Sweden, and the kobellite homologous series. Canadian Mineralogist, 24, 7–18.

Zimmermann, H., Carpenter, C.D., and Nitsche, R. (1975) The crystal structure of bismuth thiophosphate $BiPS_4$. Acta Crystallographica, B31, 2003–2006.

Zucker, U.H., Perenthaler, E., Kuhs, W.F., Bachmann, R., and Schulz, H. (1983) PROMETHEUS, a program system for investigation of anharmonic vibrations in crystals. Journal of Applied Crystallography, 16, 358.

MANUSCRIPT RECEIVED SEPTEMBER 3, 1986
MANUSCRIPT ACCEPTED FEBRUARY 13, 1987